2021 43rd Annual International Conference of the
IEEE Engineering in Medicine & Biology Society (EMBC)
Oct 31 - Nov 4, 2021. Virtual Conference

Simulation of impedance control applied to lower limb exoskeletons: assessment of its effectiveness in assisting disabled people during gait swing phase

Denis Mosconi[1] and Adriano A. G. Siqueira[2], *Member, IEEE*

Abstract— **In this work we are interested in to assess the effectiveness of a impedance control applied to a lower limb exoskeleton that assists a individual with weakness to perform the swing movement of gait. To this, we carried out simulations using a human-exoskeleton interaction model from OpenSim, a forward dynamics-based simulation algorithm from MATLAB and experimental data from a subject walking on a treadmill. The results proved that the control is efficient and capable of providing the necessary complementary torque so that the person can complete the movement with dexterity.**

I. INTRODUCTION

In the last decades, the research in the field of robot-assisted rehabilitation of stroke victims has increased. This is due the fact that the number of motor impaired people in consequence of stroke is also increasing continuously. According to the World Health Organization, almost 15 million people are victimized by stroke each year. A third of these remains with motor impairment [1], [2].

In order to meet this demand, several rehabilitation robots have been developed [3], [4], [5], [6]. Some advantages of using these robots include reducing the number of therapists per patient (especially in gait rehabilitation, which can require up to three therapists), making qualified labor more disposable, increasing the frequency and repeatability of rehabilitation exercises, active participation of the patient and acquisition of data that enable a prognosis with greater objectivity [7], [8].

While there are several scientists and engineers focused on the development of rehabilitation robots, a further portion of these researchers strive to develop controllers for such machines in order to ensure that they will interact with users in a safe and efficient manner, not putting the patient at risk and nor compromising the good development of the therapy. Many of these controls are based on the impedance control proposed by Hogan [9] and seek to satisfy the prerequisites for efficiency and safety and thus, together with the robots, compose a set of useful tools for the rehabilitation of stroke victims.

Both the design of robots and their controllers involve high complexity, since the robot-user set is a system composed of non-linearities and parameters that are difficult to measure or even estimate (e.g. friction in the robot joints and torque in the articulations of the patient). Thus, in order to make the development of such controllers less costly (both in terms of time and financial resources), computational resources have been used [10], [11], [12], [13]. Thus, using simulations to verify the effects of interaction controls applied to rehabilitation robots is essential for the agile and safe development of such controls.

The objective of this work is to simulate the effects of a impedance control applied to a lower limb exoskeleton used by a weakness subject and asses it effectiveness. The impedance control intends to help the subject to perform well the swing movement during a gait step, by applying an auxiliary torque to the joints of the hip and knee.

Following the scientific method, a hypothesis is proposed: the impedance control is capable of providing the necessary torque for a weakness subject to be able to perform the swing movement during gait.

This type of study is justified by the fact that it is important to analyze how the impedance control can contribute to assist weakened patients who are rehabilitating the swing gait movement. It is expected that this type of controller will be able to assist exoskeleton users to perform the movements with more dexterity, providing the necessary torque to maintain the amplitude and pattern of the movement, factors that can be analyzed through the simulations. In addition, it is also possible to determine what are the best gains of the controller for a given type of anthropometry and subject weakness level, since the simulations allow to do this easily and quickly, without putting both the patient and the equipment at risk.

II. METHODOLOGY

The methodology of this work can be divided into three parts: experimental procedure, simulation and analysis of the results. Each of these parts are presented in detail below.

A. Experimental Procedure

The first stage of the experimental procedure was the collection of anthropometric data from the health male 29-year-old subject who performed the experiments. Such data are basically the height and mass (1.77 m and 84 kg in this case, respectively) and were used to fit the computational model to the individual.

The second stage comprises the subject wearing the exoskeleton ExoTAO and walking on a treadmill at a speed of 2

Funding agency: CAPES.
[1]Denis Mosconi is with the Mechanical Engineering Department, University of São Paulo, São Carlos, Brazil. denis.mosconi@ifsp.edu.br
[2]Adriano A. G. Siqueira with the Mechanical Engineering Department, University of São Paulo, São Carlos, Brazil. siqueira@sc.usp.br

978-1-7281-1178-0/21/$31.00 ©2021 IEEE

km/h for 3 minutes. The ExoTAO (Fig. 1) is a modular lower limb exoskeleton developed by [4] and is composed of six free and independent joints that allow movements of flexion and extension of the hip, knee and ankle. Such joints are connected by telescopic lightweight tubular links that allow the exoskeleton be used by patients with body height between 1.65 and 1.90 m. The hip and ankle joints are equipped with an absolute encoder AksIM™ (from Renishaw), and the knee joint is appareled with a series elastic actuator (SEA) designed by [14]. In this stage, no torque was applied by the ExoTAO and the angular position from the hip and knee joints were measured, processed, filtered and made available to be used in the simulations.

Fig. 1. A subject wearing the exoskeleton ExoTAO.

B. Simulation

To perform the simulations, first a computational human-exoskeleton interaction model was fitted to the subject, using the anthropometric data from the experimental procedure. The interaction model is composed of a computational model of the neuromusculoskeletal system of a human leg, *leg6dof9musc*, provided by OpenSim[1], in whose articulations (only hip and knee, in this work) were added coordinate actuators in order to reproduce the joint actuators from the exoskeleton. The ankle joint was maintained at 90 degrees. To fit the interaction model to the subject, the *Scale Tool* from OpenSim was used. At this point it is important to tell that OpenSim is an open-source platform developed by [15] that provides tools and 3D models for modeling, simulating and analyzing movements related to the human neuromusculoskeletal system.

After adjusted the interaction model to the subject, the *Inverse Dynamics Tool* from OpenSim was used to determine the joint torques necessary to perform the movement accomplished by the human walking on the treadmill and measured with the sensors of the ExoTAO. As we are interested in simulate a human with some weakness, the torques determined with the *Inverse Dynamics Tool* were reduced in order to emulate such weakness. As no Ground Reaction Forces measurement were made, only the swing phase of the right leg was considered during the gait movement.

[1]http://opensim.stanford.edu

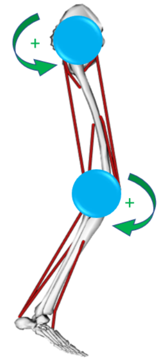

Fig. 2. Leg6dof9musc: a three-dimensional, 6 degree-of-freedom model with 9 musculotendon actuators model of a human leg. The red lines represent the muscles and the green arrows denote the orientation of joint movements. The blue lines represent the actuators of the ExoTAO.

As in the simulations the interaction model represents a subject with weakness and unable to perform the desired movement, it is necessary that the exoskeleton provides a complementary torque in order to help the user to develop the movement deftly. This complementary torque provided by the exoskeleton is determined by an impedance control, whose law is described by equation (1).

$$\begin{bmatrix}\tau_H \\ \tau_K\end{bmatrix} = \begin{bmatrix}K_H & 0 \\ 0 & K_K\end{bmatrix}\begin{bmatrix}e_H \\ e_K\end{bmatrix} - \begin{bmatrix}B_H & 0 \\ 0 & B_K\end{bmatrix}\begin{bmatrix}\dot{\theta}_H \\ \dot{\theta}_K\end{bmatrix} \quad (1)$$

In the variables of the equation above, the subscripts H and K refer to hip and knee, respectively. τ_i is the torque provided by the exoskeleton (where $i \in \{H, K\}$). K_i is the virtual stiffness and B_i is de virtual damping coefficient of the robot. $\dot{\theta}_i$ is the angular velocity of the joint and e_i is the position error described by equation (2).

$$\begin{bmatrix}e_H \\ e_K\end{bmatrix} = \begin{bmatrix}\theta_H^d \\ \theta_K^d\end{bmatrix} - \begin{bmatrix}\hat{\theta}_H \\ \hat{\theta}_K\end{bmatrix} \quad (2)$$

Above, the θ_i^d refers to the desired movement to be accomplished, that in this case is the movement performed by the subject walking on the treadmill (remember: this subject is a healthy person and the model simulated represents a person with weakness, then it is desired that, when helped by the exoskeleton, the model simulated performs the same movement as a healthy person). $\hat{\theta}_i$ is the movement performed by the computational interaction model during the simulation.

In this work, the values of the virtual stiffness and damping coefficient where determined through trial and error.

The simulations were performed using a forward dynamics-based algorithm developed in MATLAB® (Fig. 3). This algorithm applies to the interaction model the torques from the controls and/or experimental measurements, then realizes numerical integration from which results the movement performed by the model ($\hat{\theta}$). In this case, the torques applied to the model are the user torquer (τ_{user}) and the exoskeleton torque (τ_{exo}), both torques are based on the desired movement (θ^d). In Fig. 3, the *User Control* block consists of a routine that, in each iteration of the algorithm, decreases the estimated torque (τ_{ID}) in order to simulate the user weakness, so that the user torque is always less than necessary to complete the movement ($\tau_{user} < \tau_{ID}$). The equation (3) shows the function that determines the τ_{user} through the τ_{ID}.

$$\tau_{user} = \rho\tau_{ID} \tag{3}$$

Where ρ is determined as:

$$\rho_k = \alpha\rho_{k-1} + (1-\alpha)rand(0,1) \tag{4}$$

In this case we used $\alpha = 0.85$ in order to provide a smooth variation of ρ.

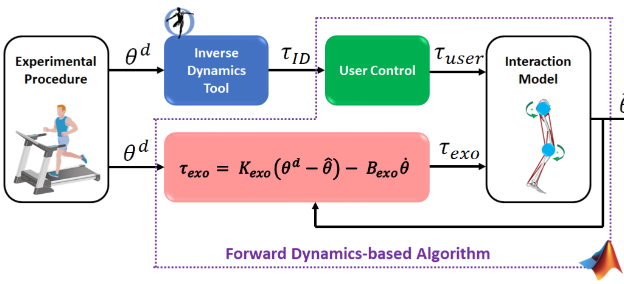

Fig. 3. Flowchart of the methodology and the forward dynamics-based algorithm applied in this work.

Both the human-exoskeleton interaction model and the forward dynamics-based algorithm were developed and validated in previous works [16]. In the present work we are interested in use them as a tool to simulate a interaction control.

All simulations were carried out on a computer with Intel®Core™i7-5500 2.40 GHz processor, 8.00 GB of RAM, 2.00 GB dedicated video card, Windows 10 Home Single Language 64 bits. The OpenSim version 3.3 and the MATLAB R2017b were the platforms where the simulations took place.

C. Analysis

In order to assess the effectiveness of the impedance control, two type of simulations were performed: one with the interaction model helped by the exoskeleton and other with only the interaction model, without the help from the robot.

As the interaction model represents a subject with weakness, it is expected that the model can not to perform the movement well, then without the robot the expected result is $\hat{\theta} \neq \theta^d$. The purpose of the use of the robot is to help the user to perform well the desired movement, then with the exoskeleton guided by the impedance control, the expected result is $\hat{\theta} \approx \theta^d$. To verify this results, an analysis comparing the angular position obtained with the simulations and the ones obtained through the experimental procedure was made.

It is know that through the *Inverse Dynamics Tool* the necessary torque to perform the movement (τ_{ID} in the Fig. 3) is determined. Then, to the model perform the desired movement, it need develop this torque, which is not possible since such model represents an weakness subject. Then it is expected that the impedance control promotes the complementary torque, through the exoskeleton, to ensure that the model will be provided with the necessary torques to accomplish the movement. Then, it is expected that:

$$\tau_{exo} = \tau_{ID} - \tau_{user} \tag{5}$$

To verify this results, a comparison between the torques was made.

We also determined a performance index as expressed by equation (6). It is expected that this index will be the lowest possible for a good performance of the control.

$$J = \sqrt{\frac{1}{N}\sum_{k=1}^{N}(\tau_{ID(k)} - \tau_{Total(k)})^2 + (\theta^d_{(k)} - \hat{\theta}_{(k)})^2} \tag{6}$$

III. RESULTS AND DISCUSSIONS

To understand the figures of this section, some considerations are necessary: in the graphs, the shadow regions limit the maximum and minimum values of the variables plotted, while the solid line is its average value. In the legends, **w/ exo** means **with exo** (i.e. the model with the exoskeleton coupled to it, helping it) and **w/o exo** means **without exo** (i.e. only the neuromusculoskeletal model exerts torque, without the help of the exoskeleton).

Figure 4 presents the hip angular position for a initial hip weakness factor $\rho_0 = 0.2$ and impedance control gains $K_H = 65$, $B_H = 6$. Observing this figure it is possible to notice that without the help of the exoskeleton, the interaction model can not to perform the desired movement well, as expected. There are a reasonable tracking error and the movement amplitude is less than the desired. With the help of the exoskeleton, that is controlled by the impedance control presented in Section II, the model could perform the desired movement with a negligible error. The oscillations are due to the random component of the subject weakness function (equation (4)).

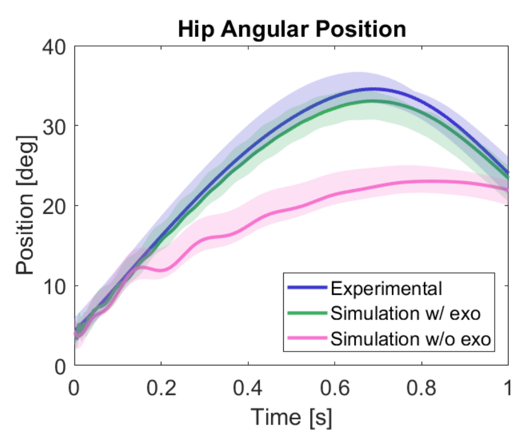

Fig. 4. Angular position of the hip.

The Fig. 5 presents the tracking error of the hip over time. The RMS error with the exoskeleton is $1.42°$ while without the exoskeleton this error is $8.32°$. The maximum errors with and without exoskeleton are $2.34°$ and $12.47°$, respectively.

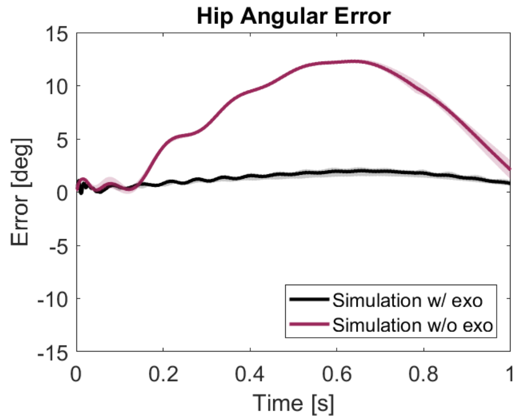

Fig. 5. Angular position error of the hip.

Figure 6 presents the hip angular position for a initial hip weakness factor $\rho_0 = 0.6$ and impedance control gains $K_K = 40$, $B_K = 3$. The same observation of the hip can be made about the knee, when we observe the Fig. 6: without the exoskeleton, the model can not to perform the movement, showing a short motion amplitude and a great tracking error. With the exoskeleton helping, the error is reduced and the amplitude is increased.

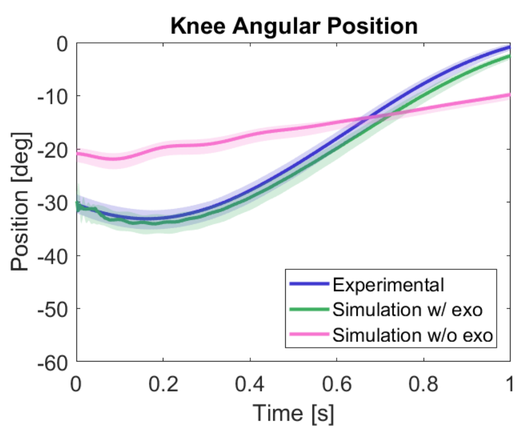

Fig. 6. Angular position of the knee.

The tracking error over time for the knee is presented in the Fig. 7. With the exoskeleton, the RMS and maximum errors are $1.58°$ and $2.22°$, respectively, while without the robot they are $8.78°$ and $12.90°$, respectively.

Analyzing Fig. 8, it is possible to verify that in fact the user executes a torque (τ_{user}) numerically lower than that necessary to perform the movement (τ_{ID}), but with a shape similar to it. It is possible to notice that the impedance control compensates the difference between the user and the necessary torques, promoting torque that when added to that of the user results in a total torque described by equation (7).

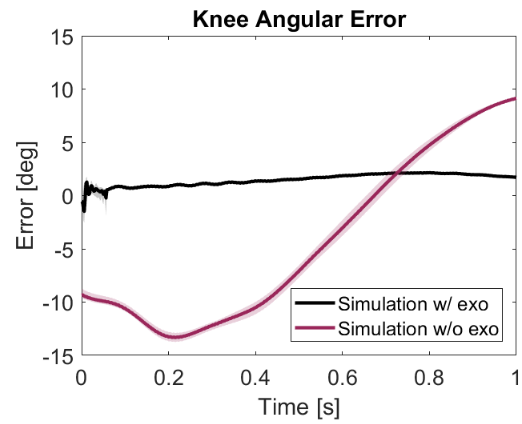

Fig. 7. Angular position error of the knee.

$$\tau_{total} = \tau_{user} + \tau_{exo} \tag{7}$$

Comparing the equations (7) and (5) we can see that they are the same, then, when observing the graphs, we expected that $\tau_{ID} \approx \tau_{total}$ if the impedance control really works, which it does, proving that the control works and is well tuned.

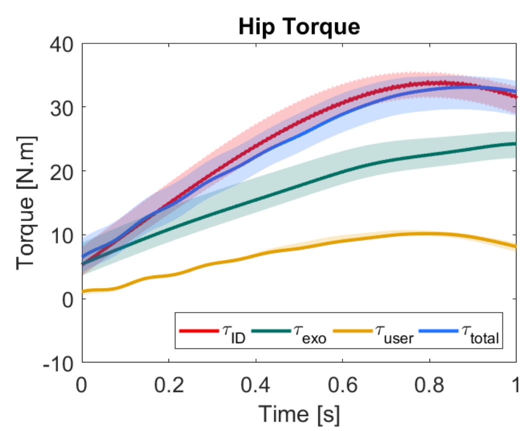

Fig. 8. Torques on the hip. The τ_{user} corresponds to the torque performed by the model of the weakness subject.

The Fig. 9 presents the absolute difference between τ_{total} and τ_{ID}, proving the effectiveness of the impedance control.

Evaluating Fig. 10, it is possible to infer that the torque developed by the user (τ_{user}) differs both numerically and in shape, from the torque required to complete the movement (τ_{ID}). In this case the impedance control provides a torque that complements the user torque both in value and shape.

The Fig. 11 presents the absolute difference between τ_{total} and τ_{ID}, proving that the impedance control was able help the user to achieve the necessary torque to perform the movement.

Some other simulations were made by varying the initial weakness factor (ρ_0) and the virtual stiffness in the exoskeleton impedance control. Analyzing the figures 12 and 13 it is possible to notice that when the virtual stiffness is increased,

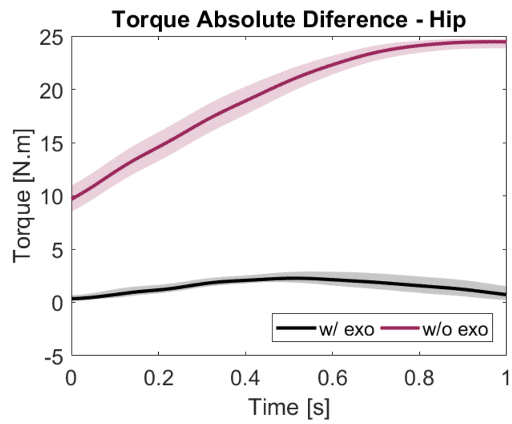

Fig. 9. Absolute difference between the necessary torque (τ_{ID}) and the total torque (τ_{total}) applied to the hip.

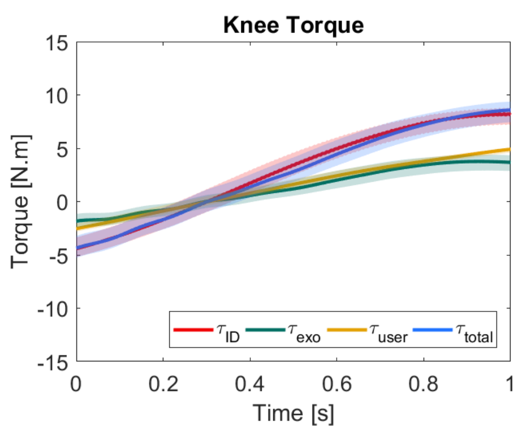

Fig. 10. Torques on the knee. The τ_{user} corresponds to the torque performed by the model of the weakness subject.

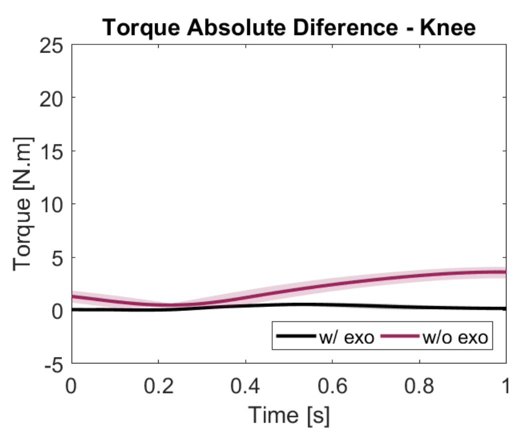

Fig. 11. Absolute difference between the necessary torque (τ_{ID}) and the total torque (τ_{total}) applied to the knee.

the position errors decrease. This is due to the increased assistance provided by the robot to the user. Obviously, for factors greater of ρ_0, the user (τ_{user}) torque will approach the necessary torque to accomplish the movement (τ_{user}) and this tends to reduce position errors.

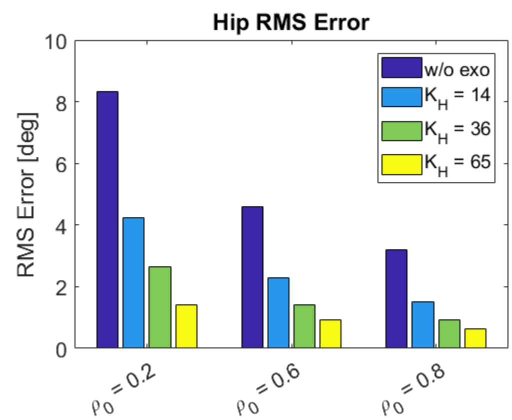

Fig. 12. Comparison between the hip position errors for some different values of ρ_0 and K_H

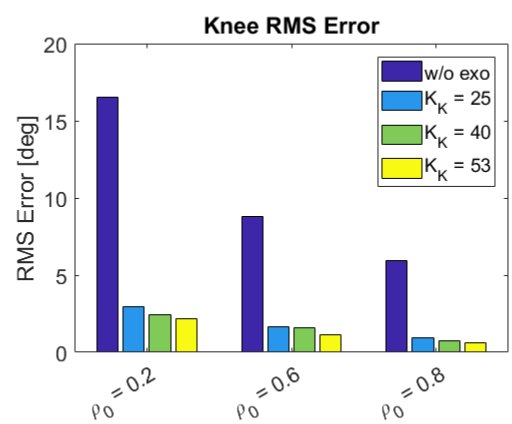

Fig. 13. Comparison between the knee position errors for some different values of ρ_0 and K_K

Analyzing the figures 14 and 15 it is possible to state that by increasing the level of assistance of the robot (by increasing virtual stiffness) the performance index tends to decrease, indicating an improvement in the quality of control (τ_{total} approaches τ_{ID}). And, for subjects with less weakness (values greater of ρ_0), the index also decreases, obviously, because $\hat{\theta}$ approaches θ^d.

About the proposed hypothesis, we can say that it is valid, since the impedance control was able to provide a complementary torque that helped the patient to execute the movement, ensuring the maintenance of the range of motion of the articulations, which is very important for the restoration of the motor skills of the patient.

With this work we were able to determine the gains of the impedance controller expressed by equation (1), for the given anthropometry, considering the user as having a weakness that incapacitates him to perform the movement

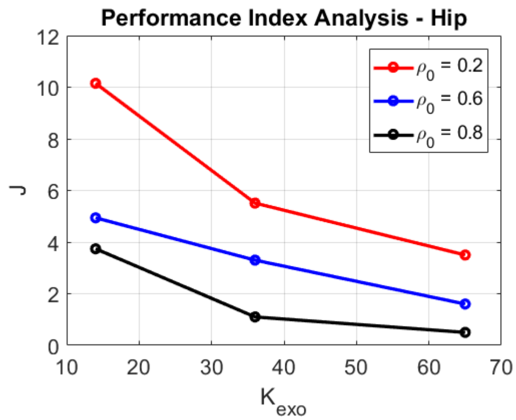

Fig. 14. Comparison between the hip performance index for some different values of ρ_0 and K_H

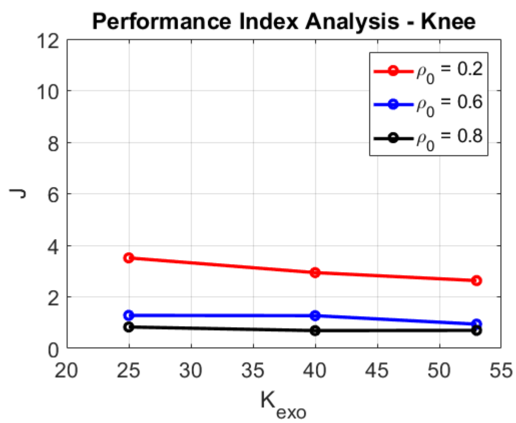

Fig. 15. Comparison between the knee performance index for some different values of ρ_0 and K_K

with dexterity. As mentioned above, the determination of such gains was made through trial and error, which was possible given the characteristic of speed and flexibility of the simulation: each simulation took no more than 10 minutes, and no one was at risk of having an accident during changes in the gains. Now it is known what are the gains that must be inserted in ExoTAO when a patient with the same anthropometry is going to use it.

IV. CONCLUSIONS

In this work, we carried out simulations of an impedance control applied to an exoskeleton that assists a subject with weakness to perform the swing phase in the gait movement.

From the results obtained it is possible to conclude that the impedance control helped the subject to perform the desired movement, with negligible tracking error, promoting the maintenance of the amplitude of motion of the user joints and providing the necessary torque, both in quantity and in shape, so that the subject could make the movement well. Finally, it can be said that impedance control is a promising tool for therapies assisted by robots.

For future work, it is intended to extend the application of this control to the complete movement of the gait, involving the phases of stance and swing, with the implication of ground reaction forces.

ACKNOWLEDGMENT

This work is supported by Pro-Rectory of Research of University of São Paulo, Coordenação de Aperfeiçoamento de Pessoal de Nível Superior - Brasil (CAPES) - Finance Code 001, PGPTA, under grant 3457/2014, and São Paulo Research Foundation (FAPESP) under grant 2013/14756-0.

REFERENCES

[1] WHO, “World health organization - world report on disability,” 2011. [Online]. Available: $http://www.who.int/disabilities/world_report/2011/report.pdf$

[2] ——, “World health organization - the top 10 causes of death,” 2018. [Online]. Available: http://www.who.int/news-room/fact-sheets/detail/the-top-10-causes-of-death

[3] P. G. Vinoj, S. Jacob, V. G. Menon, S. Rajesh, and M. R. Khosravi, “Brain-controlled adaptive lower limb exoskeleton for rehabilitation of post-stroke paralyzed,” *IEEE Access*, vol. 7, pp. 132 628–132 648, 2019.

[4] W. M. dos Santos, S. L. Nogueira, G. C. de Oliveira, G. G. Pena, and A. A. G. Siqueira, “Design and evaluation of a modular lower limb exoskeleton for rehabilitation,” in *2017 International Conference on Rehabilitation Robotics (ICORR)*. IEEE, jul 2017.

[5] A. J. Young and D. P. Ferris, “State of the art and future directions for lower limb robotic exoskeletons,” *IEEE Transactions on Neural Systems and Rehabilitation Engineering*, vol. 25, no. 2, pp. 171–182, feb 2017.

[6] W. Huo, S. Mohammed, J. C. Moreno, and Y. Amirat, “Lower limb wearable robots for assistance and rehabilitation: A state of the art,” *IEEE Systems Journal*, vol. 10, no. 3, pp. 1068–1081, sep 2016.

[7] G. J. Androwis, R. Pikar, A. Ramanujam, and K. J. Nolan, “Electromyography assessment during gait in a robotic exoskeleton for acute stroke,” *Frontiers in Neurology*, vol. 9, p. 630, 2018.

[8] A. L. Jutinico, J. C. Jaimes, F. M. Escalante, J. C. Perez-Ibarra, M. H. Terra, and A. A. G. Siqueira, “Impedance control for robotic rehabilitation: A robust markovian approach,” *Frontiers in Neurorobotics*, vol. 11, p. 43, 2017. [Online]. Available: https://www.frontiersin.org/article/10.3389/fnbot.2017.00043

[9] N. Hogan, “Impedance control: An approach to manipulation: Part 1-3,” *Journal of Dynamic Systems, Measurement, and Control*, vol. 107, pp. 1–24, 1985.

[10] A. C. C. de Sousa, J. P. C. D. Freire, and A. P. L. Bo, “Integrating hip exosuit and FES for lower limb rehabilitation in a simulation environment,” *IFAC-PapersOnLine*, vol. 51, no. 34, pp. 302–307, 2019.

[11] P. F. Nunes, W. M. dos Santos, and A. A. G. Siqueira, “Control strategy based on kinetic motor primitives for lower limbs exoskeletons,” in *10th IFAC Symposium on Biological and Medical Systems*. International Federation of Automatic Control, 2018.

[12] G. G. Peña, L. J. Consoni, W. M. dos Santos, and A. A. G. Siqueira, “Feasibility of an optimal emg-driven adaptive impedance control applied to an active knee orthosis,” *Robotics and Autonomous Systems*, no. 112, pp. 98–108, 2019.

[13] M. Khamar and M. Edrisi, “Designing a backstepping sliding mode controller for an assistant human knee exoskeleton based on nonlinear disturbance observer,” *Mechatronics*, vol. 54, pp. 121–132, 2018.

[14] W. M. dos Santos, G. A. P. Caurin, and A. A. G. Siqueira, “Design and control of an active knee orthosis driven by a rotary series elastic actuator,” *Control Engineering Practice*, vol. 58, pp. 307–318, 2017.

[15] S. L. Delp, F. C. Anderson, A. S. Arnold, P. Loan, A. Habib, C. T. John, E. Guendelman, and D. G. Thelen, “Opensim: Open-source software to create and analyze dynamic simulations of movement,” *IEEE Transactions on Biomedical Engineering*, vol. 54, no. 11, pp. 1940–1950, 2007.

[16] D. Mosconi, P. F. Nunes, I. Ostan, and A. A. G. Siqueira, “Design and validation of a human-exoskeleton model for evaluating interaction controls applied to rehabilitation robotics,” in *2020 8th IEEE RAS/EMBS International Conference for Biomedical Robotics and Biomechatronics (BioRob)*, New York, USA, 2020, pp. 629–634.